Time-Resolved Emission Spectra and Anisotropy Profiles for Symmetric Diacyl- and Dietherphosphatidylcholines

R. Hutterer,[1] F. W. Schneider,[1] and M. Hof[2,3]

The solvent relaxation behavior of Patman (6-palmitoyl-2-[[2-(trimethylammon-ium)ethyl]methylamino]naphthalene chloride) was investigated in small unilamellar vesicles composed of symmetric diacyl(1,2-dipalmitoylphosphatidylcholine; DPPC) and diether lipids (1,2-dihexadecylphosphatidylcholine; DHPC), calculating time-resolved emission spectra (TRES) and correlation functions. Both the steady-state spectra as a function of temperature and excitation wavelength and the TRES of Patman in DPPC are blue-shifted compared to those in DHPC. The solvent relaxation at three temperatures above and below the phase transition is considerably faster in DHPC than in DPPC. As the steady-state anisotropies of Patman and TMA-DPH [1-(4-trime-thylammoniumphenyl)-6-phenyl-1,3,5-hexatriene] are similar in both lipids as a function of both temperature and emission wavelength, we conclude that the introduction of ether linkages allows more efficient water penetration in the glycerol region, leading to a more polar environment and therefore faster solvent relaxation of the incorporated dyes. Using a series of n-(9-anthroyloxy) fatty acids (n = 2, 3, 6, 9, 12; 16-AP), we show that anisotropy profiles can be used to distinguish between noninterdigitated (DPPC) and fully interdigitated (DHPC) gel-phase structures. 16-(9-Antroyloxy) palmitic acid (16-AP) is an especially useful probe exhibiting pronounced differences in the steady-state anisotropies in non- and fully interdigitated gel phases.

INTRODUCTION

Although phospholipids containing ether linked alkyl or 1-alkenyl chains have been widely found in various biological systems such as mammalian cell membranes and microorganisms,[1,2] their functions are not well understood. Recent studies[3-9] have concentrated mainly on monoether lipids, which are thought to play an important role in pathobiochemistry, whereas only little work has been done on diether lipids. One

approach to understanding their biological functions is to investigate the potential change in physical membrane properties by enhanced levels of ether phospholipids,[3-9] since the absence of the carboxyl group as a hydration bond partner may change the molecular packing in the polar headgroup region.

In this work we extend our previous investigation of the solvent relaxation behavior of asymmetric diether (1-O-stearyl-2-O-lauryl-phosphatidylcholine) and diacyl lipids (1-stearoyl-2-lauroyl-phosphatidylcholine)[10] to the symmetric species DHPC and DPPC, using the polarity sensitive probe Patman (6-palmitoyl-2-[[2-(trimethylam-monium)ethyl]methylamino] naphthalene chloride).[11] We observe considerably faster solvent relaxation in DHPC, suggesting that the introduction of ether linkages allows

[1] Institute for Physical Chemistry, University of Würzburg, Marcusstr. 9/11, D-97070 Würzburg, Germany.

[2] Institute for Physical Chemistry, Charles University, Albertov 2030, CZ-12840 Prague, Czech Republic.

[3] To whom correspondence should be addressed.

more efficient water penetration in the glycerol region, leading to a more polar environment and therefore faster solvent relaxation of the incorporated dyes.

In recent years it has been recognized that, besides the classic bilayer arrangement, another gel-phase structure is possible, in which the acyl chains of opposing monolayers interdigitate. A wide variety of compounds has been reported to induce the fully interdigitated $L_\beta I$ phase in saturated like-chain phosphatidylcholines, for example, ethanol,[12-15] chlorpromazine,[16] polymyxin B,[17] and thiocyanate ions.[18] This type of interdigitation is intimitely connected with diether lipids since it is known that a fully interdigitated gel phase is adopted in the absence of any inducer in DHPC.[19-21]

For the detection of interdigitation X-ray diffraction[15,16,18,19,22,23] and neutron diffraction[24] are the most direct methods but infrared and Raman spectroscopy,[25,26] electron spin resonance,[27,28] differential scanning calorimetry (DSC),[13,19,20] NMR,[29-31] and fluorescence spectroscopy[14,32] have also been used to detect indirectly interdigitated lipid phases. However, only a few useful assays based on either pyrene[32] or DPH fluorescence[14] have been presented. The series of n-(9-anthroyloxy)fatty acids (n-AS; n = 2, 3, 6, 9, 12; 16-AP) constitutes a unique set of fluorescent dyes with a common chromophore covalently attached at different positions along the acyl chain of the fatty acid. As their chromophore is located at a defined depth in the bilayer, they are able to detect polarity and fluidity gradients in a bilayer.[33,34]

Comparing steady-state anisotropies for the series of n-(9-anthroyloxy)fatty acids in multilamellar dispersions of DPPC and DHPC, we show that anisotropy profiles can be used to distinguish noninterdigitated and fully interdigitated gel phase structures. 16-(9-Antroyloxy)palmitic acid (16-AP) proved to be an especially useful probe exhibiting pronounced differences in the steady-state anisotropies in non- and fully interdigitated gel phases.

MATERIALS AND METHODS

DPPC and DHPC were from Fluka; 6-palmitoyl-2-[[2-(trimethylammonium)ethyl]methylamino]naphthalene chloride (Patman), 1-(4-trimethylammoniumphenyl)-6-phenyl-1,3,5-hexatrien (TMA), and the n-(9-anthroyloxy)fatty acids (n-AS; n = 2, 3, 6, 9, 12; 16-AP) were purchased from Molecular Probes. The total lipid concentration was 1.0 mM for time-resolved studies and 0.1 mM for steady-state anisotropy measurements with a final lipid/dye ratio of 200:1. The solvent was removed

under a stream of N_2 and the remaining lipid–dye mixture was kept under vacuum overnight. Tris buffer (20 mM Tris, 100 mM NaCl, 10% sucrose, pH 7.5) was added and the lipid film was allowed to swell for 1 h above the phase transition temperature, with occasional vortexing to yield multilamellar vesicles (MLV). Small unilamellar vesicles (SUV) were prepared by sonication above the phase transition.

Fluorescence decays were measured from 390 to 530 nm in 10-nm steps using single-photon counting equipment (Edinburgh Instruments 199 S). Data collection (λ_{ex} = 337 nm) and data analysis were carried out as published elsewhere.[35] Mean decay times were calculated according to Ref. 36. Steady-state spectra and anisotropies (λ_{ex} = 385 nm, λ_{em} = 430 nm) were obtained using an Aminco Bowman II spectrometer. Time-resolved emission spectra (TRES) were calculated from the fit parameters of the multiexponential decays and the steady-state intensities according to Ref. 37. Correlation functions $c(t)$ were calculated from the emission maxima $v(t)$ of the TRES according to Eq. (1):

$$c(t) = \frac{v(t) - v(\infty)}{v(0) - v(\infty)} \qquad (1)$$

where $v(0)$ and $v(\infty)$ are the emission maxima (cm^{-1}) at times 0 and ∞, respectively. For comparison of different samples, average relaxation times defined by Eq. (2) were used.

$$\langle \tau_r \rangle \equiv \int_0^\infty c(t) \, dt \qquad (2)$$

RESULTS AND DISCUSSION

Solvent Relaxation in DHPC and DPPC

Steady-state emission spectra for Patman at different excitation wavelengths were recorded at three temperatures (20, 40, 52°C) below and above the phase transition temperatures T_m, which are quite similar for DPPC (41°C)[27] and DHPC (43°C).[6] Emission spectra for λ_{ex} = 360 nm in DPPC- and DHPC-SUV are compared in Fig. 1. While typical gel-phase behavior of Patman in DPPC with emission maxima around 428 nm is observed in DPPC at 20 and 40°C, the spectra in DHPC are considerably broadened and red-shifted. Above the phase transition (at 52°C) the spectra in both lipid systems are comparable but there remains a short-wavelength shoulder in DPPC not observable in DHPC. Figure 2 summarizes the emission maxima in both lipids for dif-
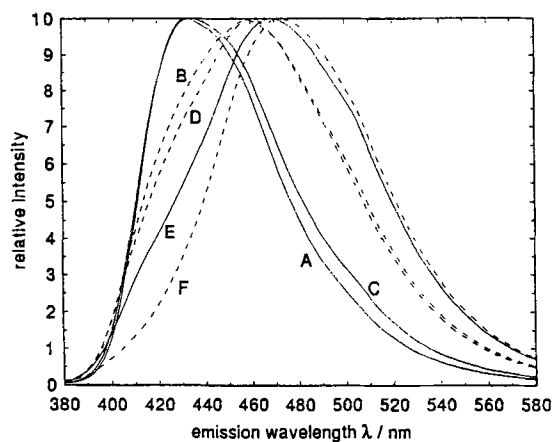
Fig. 1. Emission spectra of Patman in DPPC-SUV (solid lines, A, C, E) and in DHPC-SUV (broken lines, B, D, F) at 20, 40, and 52°C, respectively. The excitation wavelength was 360 nm.

Table I. Mean Decay Times $\langle\tau\rangle$ of Patman in DPPC- and DHPC-SUV[a]

λ_{cm} (nm)	20°C DHPC $\langle\tau\rangle$ (ns)	20°C DPPC $\langle\tau\rangle$ (ns)	40°C DHPC $\langle\tau\rangle$ (ns)	40°C DPPC $\langle\tau\rangle$ (ns)	52°C DHPC $\langle\tau\rangle$ (ns)	52°C DPPC $\langle\tau\rangle$ (ns)
390	2.18	3.21	1.60	2.43	0.80	1.14
400	2.57	3.87	1.90	2.88	1.01	1.27
410	2.99	4.38	2.18	3.38	1.40	1.50
420	3.25	4.84	2.50	3.69	1.95	1.87
430	3.47	5.04	2.88	3.92	2.54	2.31
440	3.79	5.15	3.36	4.06	3.05	2.86
450	4.02	5.22	3.77	4.34	3.38	3.36
460	4.20	5.37	4.05	4.57	3.67	3.74

[a]The errors in $\langle\tau\rangle$ are smaller than 5% of the given values in all cases. The excitation wavelength was 337 nm. Above 460 nm one decay component is always obtained with a negative preexponential factor. Monoexponential analysis yields only very small further increases in the decay times above 470 nm.
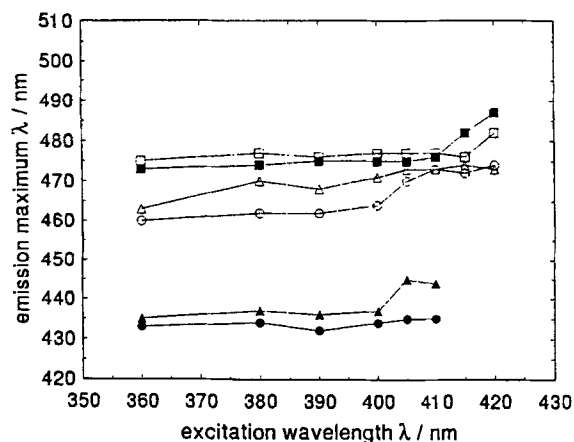

Fig. 2. Emission maxima of Patman at different excitation wavelengths in DPPC-SUV (filled symbols) and DHPC-SUV (open symbols) at 20°C (circles), 40°C (triangles), and 52°C (boxes).

ferent excitation wavelengths and temperatures. The large red shift in DHPC compared to DPPC at temperatures below T_m is obvious for all excitation wavelengths. While there is no red-edge excitation shift (REES) for Patman in DPPC at 20°C, the already red-shifted spectrum in DHPC (Fig. 1) exhibits a further shift of 13 nm on excitation at the red edge of the absorption spectrum (420 nm). The observation of REES does not give quantitative information about the rates of solvent relaxation, but the results suggest that the relaxation is faster in the diether compared to the diacyl lipid, supporting our previous results with the asymmetric lipids.[10] This points to a more polar and/or less restrictive environment of Patman in DHPC versus DPPC.

Fluorescence decays of Patman in DPPC and DHPC at different emission wavelengths (390–530 nm) were recorded at 20, 40, and 52°C. The decays could be fitted well using a biexponential model which yielded low values of χ^2 (≤ 1.2) for all emission wavelengths. For $\lambda_{cm} \geq 470$ nm one decay component was obtained with a negative preexponential factor, which is typical for the occurrence of an excited state reaction. A large increase in the mean decay times was observed with increasing λ_{cm}, as expected for increasing contributions of relaxed states. The errors in the calculated mean decay times are without exception smaller than 5% of the given values (Table I) as seen by the standard deviations of several identical experiments. Thus, they have not been itemized explicidly. For all temperatures the decay times are significantly shorter in DHPC compared to DPPC, suggesting a higher polarity of the dye environment in the diether lipid.

In Fig. 3 time-resolved emission spectra (TRES) at 20, 40, and 52°C are shown for four typical times (0.2, 0.5, 1.0, 5.0 ns) after excitation. For all temperatures considerably larger Stokes shifts are observed in DHPC than in DPPC. The relaxation rates above T_m are different but still comparable; however, below T_m the differences are quite dramatic. While there is only a small shift in DPPC at 40°C and hardly any shift at 20°C, significant shifts at these temperatures are detectable in DHPC, showing that solvent relaxation processes can still occur below the phase transition in the diether lipid. Although the calculation of a correlation function for DPPC at 20°C may be insignificant because of the small shift, it is included in Fig. 4a to visualize the slow and
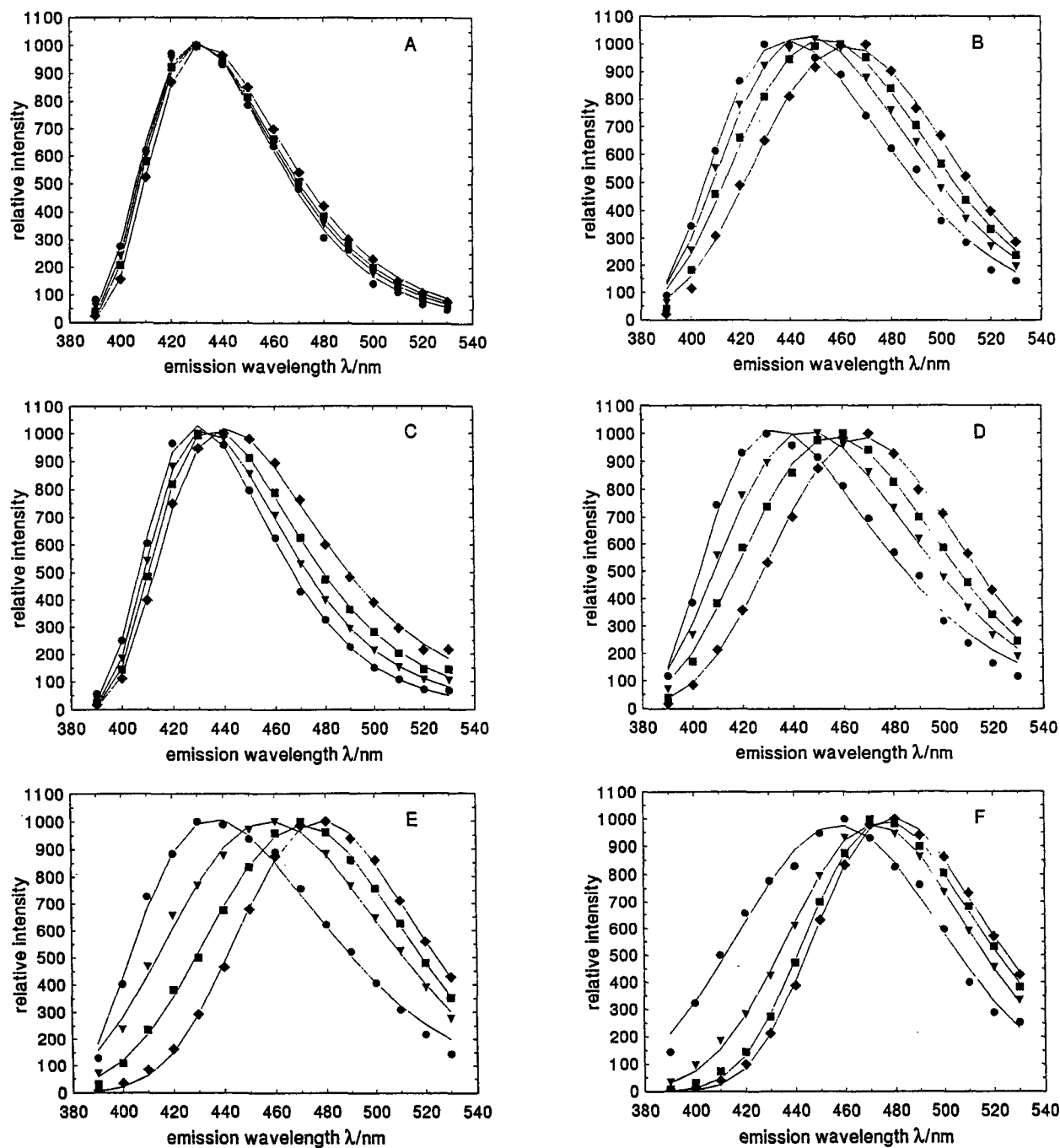
Fig. 3. Time-resolved emission spectra for Patman in DPPC- and DHPC-SUV, respectively. (A) DPPC, 20°C; (B) DHPC, 20°C; (C) DPPC, 40°C; (D) DHPC, 40°C; (E) DPPC, 52°C; (F) DHPC, 52°C. Spectra were reconstructed for t = 0.2 ns (circles), 1.0 ns (triangles), 2.0 ns (boxes), and 5.0 ns (diamonds) after excitation. The lines represent the best fits to the data points, using a log-normal lineshape function [37].

nonexponential relaxation behavior in this system. However, no relaxation time is given for this system in Table II, which summarizes the shifts and mean relaxation times calculated according to Eq. (2). In Fig. 4b the half-widths of the TRES are shown. Typically, the widths

exhibit a maximum at a time comparable to the mean relaxation time, decreasing to a value characteristic for emission from the relaxed state. Because of the slow relaxation of Patman in the DPPC gel phase, however, no maximum of $\nu_{1/2}$ is reached at 20 and 40°C; rather,
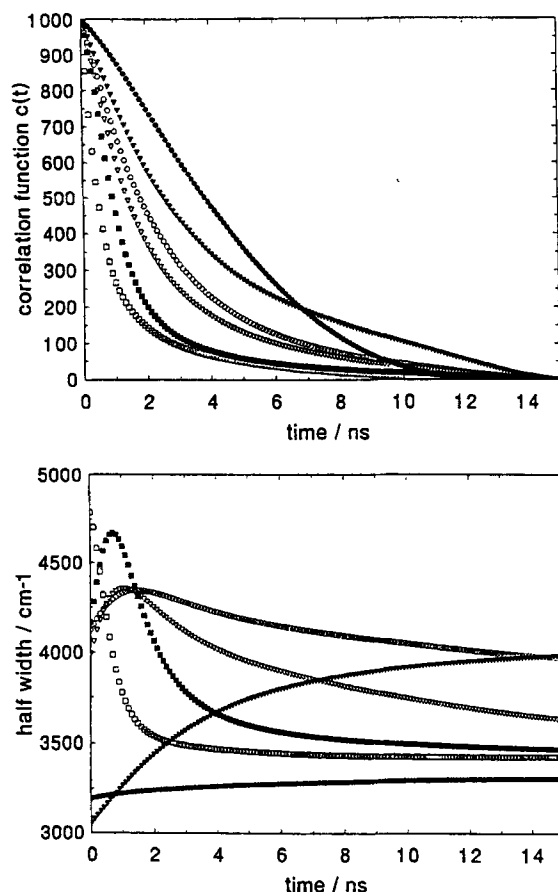
Fig. 4. Correlation functions (a), calculated according to Eq. (1), and half-widths (b) for Patman in DPPC-SUV (filled symbols) and DHPC-SUV (open symbols), respectively, at 20°C (circles), 40°C (triangles), and 52°C (boxes).

Table II. Stokes Shifts and Mean Relaxation Times $\langle \tau_r \rangle$, Calculated According to Eq. (2), for Patman in DPPC- and DHPC-SUV

Temperature (°C)	DPPC		DHPC	
	$\langle \tau_r \rangle$ (ns)	Shift (nm)	$\langle \tau_r \rangle$ (ns)	Shift (nm)
20	n.d.ᵃ	5	2.6	31
40	3.7	17	2.0	43
52	1.2	49	0.7	31

ᵃNot determined because of the small shift; see text.

the widths increase continuously. In contrast, the half-widths in DHPC at 20 and 40°C at short times after excitation are much larger, corresponding to emission from a higher number of differently relaxed states. At 52°C the relaxation is so rapid that a maximum of different states is already present at very short times after

excitation, leading to a fast decrease in the widths of the TRES with time.

Together with our previous results obtained with asymmetric diacyl and diether lipids,[10] these data clearly demonstrate that the considerably faster solvent relaxation in diether compared to diacyl lipids does not depend on the presence of asymmetric lipid chains but is due only to the different connection between the glycerol backbone and the hydrocarbon chains.

To assure that the observed differences in relaxation behavior are not caused by extremely different fluorophore mobilities in both lipid types, steady-state anisotropy measurements with TMA and Patman as a function of both temperature (λ_{em} = 430 nm) and emission wavelength (T = 20, 40, 52°C) were performed. Very similar anisotropy behavior in DPPC and DHPC was observed with both dyes for all investigated conditions (data not shown). For Patman, the anisotropy values decrease with increasing emission wavelength (especially at higher temperature), but they are nearly identical in DPPC and DHPC. Thus, the mobilities of incorporated dyes do not seem to be significantly affected by the substitution of the acyl groups by ether linkages, while the physical properties of the interface region are considerably modified, as may be concluded from the differences in solvent relaxation behavior. Our results are in agreement with NMR data which have demonstrated that DHPC molecules continue to show rapid axial diffusion at much lower temperatures than DPPC.[29]

In conclusion, TRES and steady-state spectra of Patman show clearly that the substitution of an acyl by an ether linkage favors the penetration of water and leads to a more mobile and polar headgroup domain.

## Anisotropy Profiles for Non- and Fully Interdigitated Lipids

In the second part of this work we focus on another interesting property of diether lipids by means of fluorescence spectroscopy. In contrast to MLV composed of the diacyl lipid DPPC, MLV composed of the diether lipid DHPC adopt a fully interdigitated structure below 35°C.[29] Although interdigitated phases may be most unequivocally identified using diffraction methods, a simple assay using fluorescence spectroscopy seemed desirable.

Steady-state anisotropy measurements with a set of *n*-AS dyes (2-, 3-, 6-, 9-, 12-AS; 16-AP) incorporated in MLV composed of either DPPC or DHPC were performed as a function of temperature. The steady-state anisotropies for some selected temperatures are given in Table III. All fluorophores exhibited a pronounced de-

Table III. Steady-State Anisotropy Data for the n-AS dyes in DPPC- and DHPC-SUV at Selected Temperatures[a]

Temp. (°C)	Lipid	2-AS	3-AS	6-AS	9-AS	12-AS	16-AP
10	DPPC	0.161	0.157	0.162	0.171	0.151	0.146
	DHPC	0.232	0.210	0.154	0.145	0.139	0.179
20	DPPC	0.156	0.150	0.166	0.168	0.150	0.138
	DHPC	0.215	0.212	0.150	0.151	0.133	0.159
30	DPPC	0.153	0.146	0.175	0.164	0.143	0.120
	DHPC	0.182	0.200	0.186	0.158	0.137	0.120
34	DPPC	0.152	0.143	0.179	0.160	0.133	0.102
	DHPC	0.177	0.191	0.186	0.159	0.130	0.110
38	DPPC	0.151	0.141	0.173	0.152	0.124	0.100
	DHPC	0.171	0.183	0.185	0.152	0.121	0.102
40	DPPC	0.150	0.137	0.172	0.142	0.110	0.092
	DHPC	0.168	0.174	0.181	0.147	0.113	0.098
42	DPPC	0.146	0.120	0.151	0.114	0.081	0.076
	DHPC	0.166	0.160	0.169	0.134	0.092	0.092
43	DPPC	0.124	0.109	0.114	0.880	0.064	0.037
	DHPC	0.160	0.138	0.152	0.114	0.072	0.076
50	DPPC	0.109	0.092	0.098	0.068	0.052	0.034
	DHPC	0.120	0.109	0.109	0.076	0.054	0.033

[a]The excitation wavelength was 385 nm; the emission was detected at 430 nm.
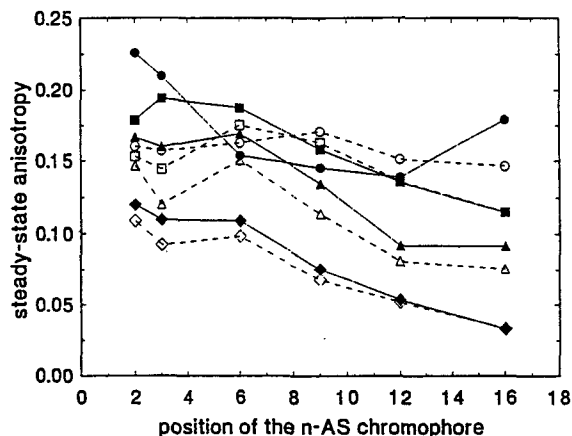
Fig. 5. Anisotropy profiles for a set of n-AS dyes in DPPC-SUV (open symbols) and DHPC-MLV (filled symbols). The excitation wavelength was 385 nm; emission was detected at 430 nm. Profiles are given for 10°C (circles), 32°C (boxes), 42°C (triangles), and 50°C (diamonds).

crease in the anisotropy (r_{ss}) values near the main phase transition, which was largest for those dyes localized closer to the bilayer center (9- and 12-AS; 16-AP). While there is a clear fluidity gradient in the liquid crystalline phase of both lipids (the r_{ss} values decrease in the order 2-AS > 3-AS ≈ 6-AS > 9-AS > 12-AS > 16-AP), the highest anisotropy in the gel phase of DPPC was found for 6-AS. In the normal gel phase provided

by DPPC, 16-AP shows the lowest r_{ss} values irrespective of temperature.

For DHPC another characteristic temperature behavior of the steady-state anisotropies of the set of n-AS dyes is observed. 2-AS shows high r_{ss} values at a low temperature (0.232) compared to the noninterdigitated phase in DPPC (0.161). Up to 30°C a continuous decrease in the anisotropy is observed. A pronounced decrease occurs at the main phase transition temperature around 43°C. The behavior of 3-AS is quite similar. For 6-AS, however, there is an increase in the anisotropy with increasing temperature up to around 32°C, followed by nearly constant r_{ss} values up to 40°C and a sharp decrease at the main phase transition. For 9-AS and 12-AS, only minor changes in the anisotropy occur between 10 and 40°C, with a sharp decrease at the phase transition. 16-AP is more restricted in the fully interdigitated phase at 10°C compared to the normal gel phase in DPPC, but there is a fast and continuous decrease in the anisotropy values up to the main phase transition, where they drop to very low values, as observed in DPPC.

The data described above have been used to construct profiles of the steady-state anisotropy versus position of the chromophore along the acyl chain for some characteristic temperatures. In Fig. 5 these profiles are compared for DPPC and DHPC. The noninterdigitated gel phase is characterized by a rise in the anisotropy from position 2 to position 6, followed by a steady decrease. Above T_m, 2-AS exhibits the highest anisotropy. A pronounced fluidity gradient from position 2 to position 16 is characteristic for the liquid crystalline phase of both lipids. A clearly different profile was obtained for the fully interdigitated phase at a low temperature (10°C). Anisotropy values are high for 2- and 3-AS and considerably lower for 6-, 9-, and 12-AS. In contrast to the noninterdigitated phase of DPPC, a considerable rise in the anisotropy is observed from 12-AS to 16-AP. This profile changes markedly at higher temperatures. At 32°C the maximal anisotropy is observed for 3-AS, followed by 6-AS, with a continuous decrease from 6-AS to 16-AP. Above T_m, the profile is similar to that for the noninterdigitated DPPC. Thus, both gel-phase types yield a different characteristic profile which seems to be of diagnostic value for determination of the packing of a specific lipid. Within this set of probes, 2-AS and 16-AP are clearly the most useful ones, showing the most different behavior in DHPC and DPPC.

We conclude that the anisotropy profiles of the n-AS dyes show characteristic differences for non- and fully interdigitated gel phases. Their extremely different behavior in MLV composed of DHPC and DPPC pro-

motes 2-AS and 16-AP to be outstanding dyes for the detection of fully interdigitated gel phases.

REFERENCES

1. F. Snyder (Ed.) (1982) *Ether Lipids: Chemistry and Biology*, Academic Press, New York.
2. F. Paltauf (1983) in H. K. Mangold and F. Paltauf (Eds.), *Ether Lipids: Biochemical and Biomedical Aspects*, Academic Press, New York, pp. 309–353.
3. D. O. Shaw and J. M. Shulman (1965) *J. Lipid Res.* **6**, 341.
3. A. Hermetter and F. Paltauf (1981) *Chem. Phys. Lipids* **29**, 225.
4. F. Paltauf, H. Hauser, and M. C. Phillips (1971) *Biochim. Biophys. Acta* **249**, 539.
5. A. Hermetter and F. Paltauf (1981) *Chem. Phys. Lipids* **29**, 225.
6. D. J. Vaughan and K. M. Keough (1974) *FEBS Lett.* **47**, 158.
7. T.-C. Lee and C. Fitzgerald (1980) *Biochim. Biophys. Acta* **598**, 189.
8. J. M. Seddon, G. Cevc, and D. Marsh (1983) *Biochemistry* **22**, 1280.
9. D. J. Siminovitch, M. J. Ruocco, and R. G. Griffin (1984) *Biophys. J.* **45**, 197a.
10. R. Hutterer, F. W. Schneider, V. Fidler, E. Grell, and M. Hof, *J. Fluoresc.* (in press).
11. J. R. Lakowicz, D. R. Bevan, B. P. Malival, H. Cherek, and A. Balter (1983) *Biochemistry* **22**, 5714–5722.
12. E. S. Rowe (1992) in R. Watson (Ed.), *Alcohol: Neurobiology and Physiology*, CRC Press, Boca Raton, FL, pp. 239–267.
13. E. S. Rowe and T. A. Cutrera (1990) *Biochemistry* **29**, 10398–10404.
14. P. Nambi, E. S. Rowe, and T. J. McIntosh (1988) *Biochemistry* **27**, 9175–9182.
15. S. A. Simon and T. J. McIntosh (1984) *Biochim. Biophys. Acta* **773**, 169–172.
16. T. J. McIntosh, R. V. McDaniel, and S. A. Simon (1983) *Biochim. Biophys. Acta* **731**, 109–114.
17. A. Theretz, J. L. Ranck, and J. F. Tocanne (1983) *Biochim. Biophys. Acta* **732**, 499–508.
18. B. A. Cunningham and L. J. Lis (1986) *Biochim. Biophys. Acta* **861**, 237–242.
19. M. J. Ruocco, D. J. Siminovitch, and R. G. Griffin (1985) *Biochemistry* **24**, 2406–2411.
20. P. Laggner, K. Lohner, G. Degovics, K. Müller, and A. Schuster (1987) *Chem. Phys. Lipids* **44**, 31–60.
21. J. T. Kim, J. Mattay, and G. G. Shipley (1987) *Biochemistry* **26**, 6592–6598.
22. S. W. Hui, J. T. Mason, and C. Huang (1984) *Biochemistry* **23**, 5570–5577.
23. J. L. Ranck and J. F. Tocanne (1982) *FEBS Lett.* **143**, 175–177.
24. L. F. Braganza and D. L. Worcester (1986) *Biochemistry* **25**, 2591–2596.
25. T. J. O'Leary and I. W. Levine (1984) *Biochim. Biophys. Acta* **776**, 185–189.
26. C. Huang, J. T. Mason, and I. W. Levin (1983) *Biochemistry* **22**, 2775–2780.
27. J. M. Boggs, G. Rangaraj, and A. Watts (1989) *Biophys. Biochim. Acta* **981**, 243–253.
28. J. M. Boggs and G. Rangaraj (1985) *Biochim. Biophys. Acta* **816**, 221–233.
29. M. J. Ruocco, A. Makriyannis, D. J. Siminovitch, and R. G. Griffin (1985) *Biochemistry* **24**, 4844–4851.
30. J. Frenzell, K. Arnold, and P. Nuhn (1978) *Biochim. Biophys. Acta* **507**, 185–197.
31. D. J. Siminovitch, K. R. Jeffrey, and H. Eibl (1983) *Biochim. Biophys. Acta* **727**, 122–134.
32. M. Yamazaki, M. Miyazu, and T. Asano (1992) *Biochim. Biophys. Acta* **1106**, 94–98.
33. K. R. Thulborn and W. H. Sawyer (1978) *Biochim. Biophys. Acta* **511**, 125–140.
34. K. R. Thulborn, L. M. Tilley, W. H. Sawyer, and F. E. Treolar (1979) *Biochim. Biophys. Acta* **558**, 166–178.
35. M. Hof, J. Schleicher, and F. W. Schneider (1989) *Ber. Bunsenges. Phys. Chem.* **93**, 1377–1381.
36. J. R. Lakowicz (1983) *Principles of Fluorescence Spectroscopy*, Plenum Press, New York.
37. M. Maroncelli and G. R. Fleming (1987) *J. Chem. Phys.* **86**, 6221–6239.